2017

Gallium Vacancies in β-Ga_2O_3 Crystals

Brant E. Kananen
Air Force Institute of Technology

Larry E. Halliburton
West Virginia University

K. T. Stevens
Northrop Grumman Synoptics

G. K. Foundos
Northrop Grumman Synoptics

Recommended Citation

Kananen, B. E., Halliburton, L. E., Stevens, K. T., Foundos, G. K., & Giles, N. C. (2017). Gallium vacancies in β-Ga2O3 crystals. Applied Physics Letters, 110(20), 202104. https://doi.org/10.1063/1.4983814

Applied Physics Letters

Gallium vacancies in β-Ga_2O_3 crystals

Cite as: Appl. Phys. Lett. **110**, 202104 (2017); https://doi.org/10.1063/1.4983814
Submitted: 22 March 2017 . Accepted: 08 May 2017 . Published Online: 18 May 2017

B. E. Kananen, L. E. Halliburton, K. T. Stevens, G. K. Foundos, and N. C. Giles

Gallium vacancies in β-Ga_2O_3 crystals

B. E. Kananen,[1] L. E. Halliburton,[2] K. T. Stevens,[3] G. K. Foundos,[3] and N. C. Giles[1,a)]
[1]*Department of Engineering Physics, Air Force Institute of Technology, Wright-Patterson Air Force Base, Ohio 45433, USA*
[2]*Department of Physics and Astronomy, West Virginia University, Morgantown, West Virginia 26505, USA*
[3]*Northrop Grumman Synoptics, 1201 Continental Blvd, Charlotte, North Carolina 28273, USA*

(Received 22 March 2017; accepted 8 May 2017; published online 18 May 2017)

The gallium vacancy, an intrinsic acceptor, is identified in β-Ga_2O_3 using electron paramagnetic resonance (EPR). Spectra from doubly ionized (V_{Ga}^{2-}) and singly ionized (V_{Ga}^{-}) gallium vacancies are observed at room temperature, without photoexcitation, after an irradiation with high-energy neutrons. The V_{Ga}^{2-} centers (with $S = 1/2$) have a slight angular variation due to a small anisotropy in the g matrix (principal values are 2.0034, 2.0097, and 2.0322). The V_{Ga}^{2-} centers also exhibit a resolved hyperfine structure due to equal and nearly isotropic interactions with the ^{69,71}Ga nuclei at two Ga sites (the hyperfine parameters are 1.28 and 1.63 mT for the ^{69}Ga and ^{71}Ga nuclei, respectively, when the field is along the a direction). Based on these g-matrix and hyperfine results, the model for the ground state of the doubly ionized vacancy (V_{Ga}^{2-}) has a hole localized on one threefold-coordinated oxygen ion. The vacancy is located at one of the three neighboring gallium sites, and the remaining two gallium neighbors are responsible for the equal hyperfine interactions. The singly ionized (V_{Ga}^{-}) gallium vacancies are also paramagnetic. In this latter acceptor, the two holes are localized on separate oxygen ions adjacent to one gallium vacancy. Their spins align parallel to give a triplet $S = 1$ EPR spectrum with resolved hyperfine structure from interactions with gallium neighbors. *Published by AIP Publishing.* [http://dx.doi.org/10.1063/1.4983814]

Gallium oxide (β-Ga_2O_3) is a wide-band-gap semiconductor with an optical band edge near 4.9 eV (~250 nm). Potential applications of this material range from transparent conducting electrodes to power electronics.[1,2] Most β-Ga_2O_3 crystals available today are n type because of the unintentional presence of silicon impurities (silicon is a shallow donor when substituting for gallium ions).[3,4] Thus far, little is known experimentally about the structure and electronic properties of other possible extrinsic donors and acceptors such as germanium, fluorine, magnesium, and zinc. Also, detailed information is not available for native donors and acceptors (i.e., oxygen vacancies and gallium vacancies).

In the present letter, electron paramagnetic resonance (EPR) is used to characterize the doubly ionized ($S = 1/2$) and singly ionized ($S = 1$) charge states of the gallium vacancy in a β-Ga_2O_3 crystal. These are the V_{Ga}^{2-} and V_{Ga}^{-} acceptors, respectively. The EPR spectra from these vacancies are observed at room temperature after an irradiation with high-energy neutrons. The angular dependence of the V_{Ga}^{2-} spectrum places the unpaired spin in a p orbital on an oxygen ion. Resolved hyperfine lines show that the unpaired spin in this center interacts equally with the nuclei (^{69}Ga and ^{71}Ga) at two neighboring Ga sites. The model that emerges from these g-matrix and hyperfine results for the doubly ionized gallium vacancy (V_{Ga}^{2-}) has the hole localized on a threefold-coordinated oxygen ion (one of the three neighboring gallium sites is the vacancy, and the remaining two gallium neighbors are responsible for the equal hyperfine interactions). The vacancy is a sixfold-coordinated gallium site. In the future, advanced density-functional-theory (DFT) studies are expected to provide refinements to this V_{Ga}^{2-} model (e.g., lattice relaxation and charge delocalization).[5–8]

The β-Ga_2O_3 crystal used in the present study was grown by the Czochralski method at Northrop Grumman Synoptics (Charlotte, NC). An iridium crucible was utilized, and the growth atmosphere was a mixture of Ar, CO_2, and O_2. The growth rate was 1.5 mm/h. The structure of β-Ga_2O_3 crystals is monoclinic, and the space group is C2/m (C_{2h}^3). Lattice constants[9,10] are $a = 12.214$ Å, $b = 3.0371$ Å, $c = 5.7981$ Å, and $\beta = 103.83°$. There are two inequivalent gallium sites and three inequivalent oxygen sites in β-Ga_2O_3. The Ga(I) ions are at tetrahedral sites (with four oxygen neighbors) and the Ga(II) ions are at octahedral sites (with six oxygen neighbors). The O(I) and O(II) ions have three gallium neighbors and the O(III) ions have four gallium neighbors. We use the labeling scheme introduced by Geller.[9] Figure 1 shows a ball-and-stick representation of a unit cell in the β-Ga_2O_3 crystal.

The EPR spectra were taken at room temperature using a Bruker EMX spectrometer (the microwave frequency was near 9.85 GHz). Approximate dimensions of the EPR sample were $3.0 \times 1.5 \times 5.0\,mm^3$. Static magnetic fields were measured using a Bruker nuclear magnetic resonance (NMR) teslameter. The only EPR spectra initially present in the as-grown crystal were from shallow donors and trace amounts of Fe^{3+} and Cr^{3+}. To produce the gallium vacancies, the β-Ga_2O_3 crystal was neutron-irradiated at the Ohio State University Research Reactor (Columbus, OH). The crystal was held for 3 h in the central irradiation facility of the reactor where the total flux was $\sim 2.1 \times 10^{13}$ neutrons $cm^{-2}s^{-1}$ and the thermal flux was $\sim 1.3 \times 10^{13}$ neutrons $cm^{-2}s^{-1}$. Although not measured during the irradiation, the temperature of the crystal is estimated to have remained below 150 °C. An important effect of the neutron irradiation is the lowering of the Fermi level in the crystal

a)Author to whom correspondence should be addressed: Nancy.Giles@afit.edu

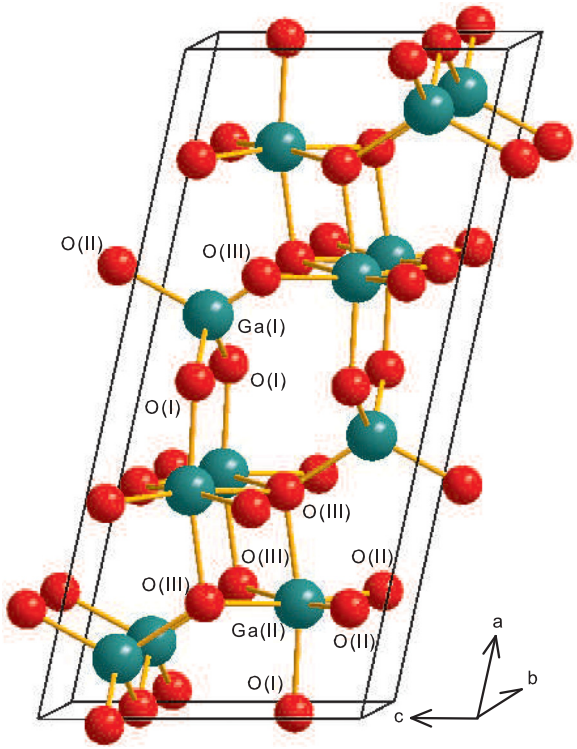

FIG. 1. Schematic representation of a unit cell in β-Ga_2O_3. Gallium ions are shown in green and oxygen ions are shown in red. The two inequivalent gallium sites, Ga(I) and Ga(II), and the three inequivalent oxygen sites, O(I), O(II), and O(III), are labeled. The types of oxygen ions around each gallium site are indicated.

as significant concentrations of gallium-vacancy acceptors are formed by momentum-conserving displacement events.[11] A lower Fermi level allows the V_{Ga}^{2-} and V_{Ga}^{-} charge states of the gallium vacancies to be observed without photoexcitation. Effects of the transmutation of Ga to Ge, occurring as a result of the irradiation, were not observed using EPR.

Figure 2(a) shows the EPR spectrum from the doubly ionized gallium vacancy (V_{Ga}^{2-}) in the neutron-irradiated β-Ga_2O_3 crystal. These data were obtained at room temperature with the magnetic field along the *a* direction. The V_{Ga}^{2-} acceptor ($S = 1/2$) has a spectrum consisting of a symmetrical set of partially resolved hyperfine lines of differing intensities (more intense in the center and less intense at the higher and lower fields) due to interactions with nearby ^{69}Ga and ^{71}Ga nuclei. Both of these isotopes have $I = 3/2$ nuclear spins, but their natural abundances and magnetic moments are measurably different. The ^{69}Ga and ^{71}Ga are 60.1% and 39.9% abundant, respectively, and their magnetic moments[12] are $^{69}\mu = +2.0166\beta_n$ and $^{71}\mu = +2.5623\beta_n$. As illustrated by the stick diagrams above the spectrum in Fig. 2(a), the complex hyperfine pattern is explained by having the unpaired spin in the V_{Ga}^{2-} acceptor interact equally with the nuclei at two gallium sites. There are three combinations of the two Ga isotopes that give rise to the observed hyperfine pattern: they are (i) two ^{69}Ga nuclei, (ii) one ^{69}Ga nucleus and one ^{71}Ga nucleus, and (iii) two ^{71}Ga nuclei. Each of these combinations is represented in a separate stick diagram above the experimental spectrum (the relative lengths of the vertical lines in the diagrams reflect the natural abundances of the two isotopes). For example, the uppermost stick diagram shows the seven lines (with relative intensities of 1:2:3:4:3:2:1) that are produced when the unpaired spin interacts equally with two ^{69}Ga nuclei. The lowest stick diagram in Fig. 2(a) is the sum of the three upper stick diagrams and thus should be directly compared to the experimental spectrum.

In Fig. 2(a), the set of seven lines produced by the equal interactions of the unpaired spin with two ^{71}Ga nuclei (i.e., the red stick diagram) provides a method to precisely determine values of hyperfine parameters. The outermost lines in this set are isolated, with little interference from other lines. Their separation, divided by six, gives the hyperfine parameter for ^{71}Ga. Scaling the result for the difference in magnetic moments then gives the related value for ^{69}Ga. These lowest and highest lines in the ^{71}Ga-^{71}Ga portion of the spectrum in Fig. 2(a) are near 346.00 and 355.75 mT. This yields values

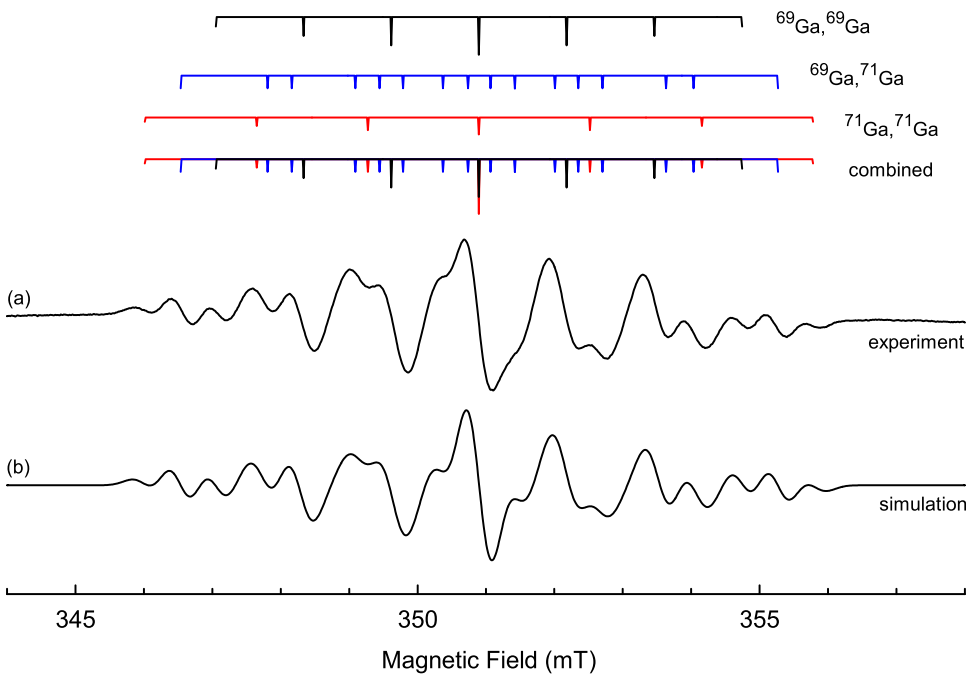

FIG. 2. (a) The EPR spectrum from the $S = 1/2$ doubly ionized gallium vacancy (V_{Ga}^{2-}) in β-Ga_2O_3. These data were taken at room temperature after a neutron irradiation. The microwave frequency was 9.8389 GHz, and the magnetic field was along the *a* direction. Above the spectrum, stick diagrams identify individual hyperfine lines arising from interactions with gallium nuclei at two neighboring gallium sites. (b) Simulated EPR spectrum using the Bruker SimFonia program.

TABLE I. *g* values and hyperfine parameters describing the EPR spectra from the doubly ionized gallium vacancy (V_{Ga}^{2-}) when the magnetic field is along each of the three crystallographic axes. The ^{69}Ga and ^{71}Ga parameters refer to interactions with individual nuclei at the two neighboring gallium sites. The estimated error is ±0.0002 for the *g* values and ±0.01 mT for the hyperfine values.

		Hyperfine parameters (mT)	
Direction of magnetic field	*g* value	^{69}Ga	^{71}Ga
a crystal axis	2.0034	1.28	1.63
b crystal axis	2.0322	1.44	1.82
c crystal axis	2.0097	1.36	1.73

of 1.28 and 1.63 mT for the ^{69}Ga and ^{71}Ga parameters, respectively, when the magnetic field is along the *a* direction. The simulated spectrum in Fig. 2(b) was created with the SimFonia program from Bruker by using these 1.28 and 1.63 mT hyperfine parameters and a linewidth of 0.327 mT. The two spectra (experimental and simulated) are in excellent agreement, thus confirming our explanation of the observed hyperfine pattern. Similar measurements of the EPR spectra taken with the magnetic field along the other crystallographic directions show that the ^{69}Ga and ^{71}Ga hyperfine matrices are nearly isotropic. This indicates that the unpaired spin density on the two neighboring ions is primarily in Ga 4*s* orbitals. Values of the Ga hyperfine parameters for the three crystallographic directions are listed in Table I.

The *g* matrix for the V_{Ga}^{2-} acceptor has a small, but easily measured, anisotropy. Figure 3 shows the angular dependence of the center EPR line when rotating the direction of the magnetic field from *a* to *b*, *b* to *c*, and *c* to *a** in increments of 15°. The space group for β-Ga_2O_3 allows two crystallograpically equivalent, but magnetically inequivalent, orientations for a defect. Site splitting, however, was not observed in the angular dependence of the V_{Ga}^{2-} center. The *a* and *c* directions are not 90° apart in the monoclinic structure; thus, an *a** direction is introduced that is 90° from *b* and *c*. The angular

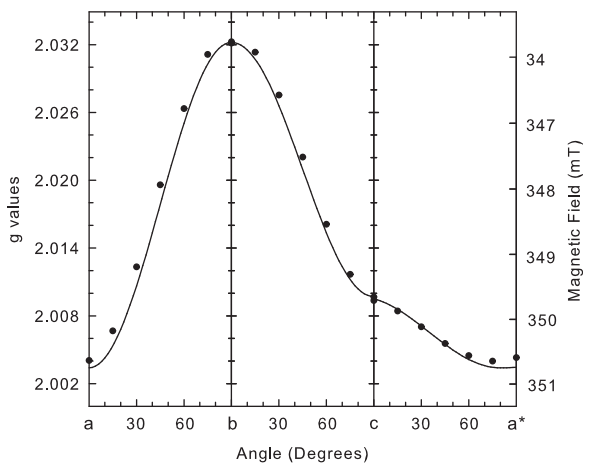

FIG. 3. Angular dependence of the *g* matrix. The change in the position of the center line of the V_{Ga}^{2-} acceptor is shown for rotations in three planes. The discrete points are experimental results, and the solid curves are computer-generated using the *g* values listed in Table I. Magnetic field values along the right vertical axis correspond to a microwave frequency of 9.835 GHz.

dependence in Fig. 3 is described by the electron Zeeman term in the spin Hamiltonian ($H = \beta \mathbf{S}\cdot\mathbf{g}\cdot\mathbf{B} + \sum(\mathbf{I_i}\ \mathbf{A_i}\ \mathbf{S})$). There are turning points in Fig. 3 along the *b* direction and near the *a** direction. In the *c* to *a** plane, the observed turning point is approximately 10° from *a** (which means that the turning point is near *a*). This places the principal axes of the *g* matrix approximately along the crystallographic *a*, *b*, and *c* directions. The corresponding *g* values (i.e., the principal values of the *g* matrix) are listed in Table I. These values were used to generate the solid curves in Fig. 3.

The small and positive *g* shifts observed for the V_{Ga}^{2-} acceptor agree with a model that has the unpaired spin (i.e., the hole) primarily located in a p_z orbital on an oxygen ion adjacent to the gallium vacancy. As described in the earlier analysis of a similar defect in $LiAlO_2$ crystals,[13] the oxygen with the hole is an O^- ion with a $2p^5$ configuration ($2p_x^2 2p_y^2 2p_z$). The threefold orbital degeneracy of this ^{2}P state ($L = 1$, $S = 1/2$) is removed by the local crystalline electric field, thus forming three energy levels (E_1, E_2, and E_3). E_1 is the ground state with the hole in the p_z orbital, whereas E_2 and E_3 are excited states with the hole in the p_x and p_y orbitals of the ion, respectively. The spin-orbit interaction mixes these excited states with the ground state and gives the following first-order expressions for the expected principal *g* values:[14]

$$g_a = g_e, \quad g_b = g_e - \frac{2\lambda}{E_2 - E_1}, \quad g_c = g_e - \frac{2\lambda}{E_3 - E_1}. \quad (1)$$

In these equations, g_e is 2.0023 (for a "free" electron) and λ is the spin-orbit coupling constant for an O^- ion. The value of 2.0034 for g_a in Table I is close to 2.0023, which indicates that the p_z orbital containing the unpaired electron spin is oriented nearly along the *a* direction in the crystal. Bartram *et al.*[15] have determined that the value of the spin-orbit coupling constant λ for an O^- ion is $-135\ cm^{-1}$. The negative sign for λ gives rise to the observed positive *g* shifts (i.e., *g* values greater than 2.0). Substituting the measured *g* values for the *b* and *c* directions from Table I into the above equations gives $E_3 - E_1 = 36480\ cm^{-1}$ and $E_2 - E_1 = 9030\ cm^{-1}$. These values of $E_3 - E_1$ and $E_2 - E_1$ only represent crystal-field splittings and are not necessarily good predictors of peak positions of possible optical absorption bands.[16]

A schematic model of the doubly ionized gallium vacancy (V_{Ga}^{2-}) is shown in Fig. 4. The hole is localized on a threefold oxygen ion at an O(I) site, and the gallium vacancy is at the neighboring sixfold Ga(II) site. The oxygen p_z orbital containing the unpaired spin (blue in Fig. 4) points toward the Ga vacancy. This orientation allows the hole to avoid its positive neighbors as much as possible, thus minimizing the total energy of the defect. The unpaired spin interacts primarily with the gallium ions at the two equivalent sites labeled Ga_A(I) and Ga_B(I). Principal-axis directions of the *g* matrix in Table I (and Fig. 3) agree with this model. One principal axis is near the unique direction of the p_z orbital (along the *a* direction toward the vacancy), another axis is parallel to the line joining the Ga_A and Ga_B neighbors (the *b* direction), and the remaining axis is perpendicular to the p_z orbital (near the *c* direction). Although not yet established, significant lattice distortion within this model is

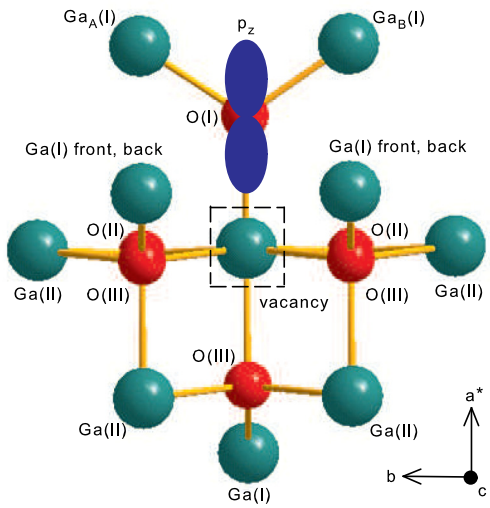

FIG. 4. Model of the doubly ionized gallium vacancy (V_{Ga}^{2-}) in β-Ga_2O_3. This view is looking back along the c axis (i.e., a projection on the plane perpendicular to the c axis). An unpaired spin (the hole) is localized in a p_z orbital on a threefold oxygen ion, O(I), adjacent to a gallium vacancy (dashed square) at a sixfold Ga(II) site. The primary hyperfine interactions are with the two equivalent gallium ions labeled Ga_A(I) and Ga_B(I).

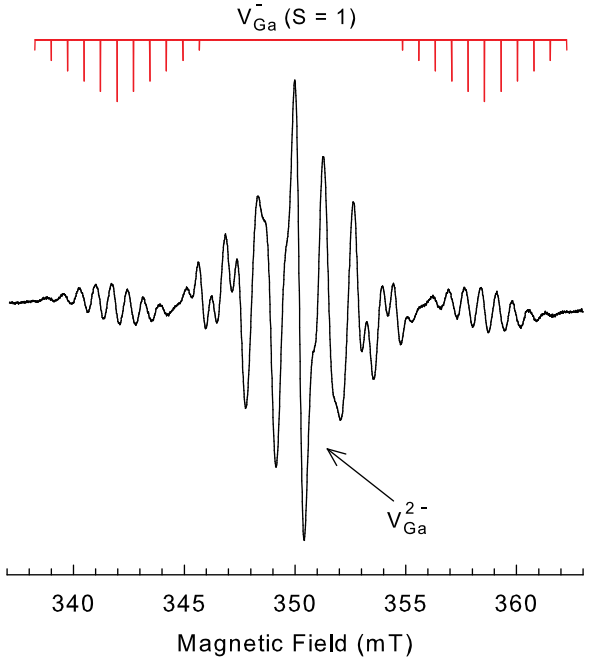

FIG. 5. The EPR spectrum from the S = 1 singly ionized gallium vacancy (V_{Ga}^{-}) in β-Ga_2O_3. The signal from the V_{Ga}^{2-} acceptor is present in the middle portion of this spectrum while lines from the V_{Ga}^{-} acceptor are seen in the high and low magnetic field regions. The microwave frequency was 9.8306 GHz, and the direction of the magnetic field was approximately midway between the a and c directions. A stick diagram above the spectrum identifies gallium hyperfine lines.

expected, with the oxygen ion with the unpaired spin (i.e., the hole) possibly moving 0.1–0.2 Å or more. We note that an EPR spectrum from a gallium vacancy at a fourfold Ga(I) site was not seen in our experiments. If Ga(I) vacancies are formed during the irradiation, our results suggest that they are in a nonparamagnetic charge state at room temperature.

Singly ionized gallium vacancies (V_{Ga}^{-}) are also observed in the β-Ga_2O_3 crystal after the neutron irradiation. In this charge state of the acceptor, two holes are located at separate oxygen ions next to one gallium vacancy. The two holes are weakly coupled (via exchange and dipole-dipole interactions) and form a triplet S = 1 state that can be detected with EPR. Figure 5 shows the spectrum from the V_{Ga}^{-} acceptor. The data were taken at room temperature with the direction of the magnetic field approximately halfway between the a and c directions in the a–c plane. In this spectrum, the S = 1 defect has two sets of lines, in the low and high magnetic field regions, that are separated by about 16.7 mT (this is the maximum separation observed for any orientation of magnetic field). The S = 1/2 spectrum from the V_{Ga}^{2-} charge state of the gallium vacancy is in the center region of Fig. 5 and is very close to the midpoint of the two S = 1 sets of lines. Thus, the spectra from the V_{Ga}^{2-} and V_{Ga}^{-} acceptors have the same g value for this direction of the magnetic field. Also, the separations between adjacent ^{69}Ga and ^{71}Ga hyperfine lines in the two spectra in Fig. 5 differ by a factor of two. The average of the ^{69}Ga and ^{71}Ga hyperfine parameters for the S = 1/2 spectrum is 1.48 mT, while the spacing of the lines in the S = 1 spectrum is 0.73 mT.

Earlier work[17,18] has shown that when two S = 1/2 defects weakly couple to form an S = 1 defect, the resulting triplet EPR spectrum has an averaged g matrix $\mathbf{g} = \frac{1}{2}(\mathbf{g_1} + \mathbf{g_2})$ and hyperfine spacings that are reduced by a factor of two ($\mathbf{A} = \frac{1}{2}\mathbf{A_1} = \frac{1}{2}\mathbf{A_2}$). Both of these features are clearly seen in the S = 1 spectrum in Fig. 5, and, together, they strongly support a model for the singly ionized gallium vacancy V_{Ga}^{-} where the two holes are localized separately on opposing oxygen ions adjacent to one gallium vacancy. If each hole interacts primarily with the Ga nuclei at its two neighboring Ga sites, a total of 13 hyperfine lines are expected[18] in each of the S = 1 sets of lines in the low and high magnetic field regions of Fig. 5. Nine lines can be seen in each of these sets in Fig. 5, with the intensities of the remaining lines below the noise level. Based on the model in Fig. 4, a V_{Ga}^{2-} acceptor converts to a V_{Ga}^{-} acceptor by localizing a second hole on the oxygen ion, O(III), at the bottom of the figure, opposite to the initial hole at the top of the figure. The two holes in the resulting V_{Ga}^{-} acceptor would be approximately 4.0 Å apart in the unrelaxed lattice (the expected lattice relaxation will likely increase this separation). Assuming only a magnetic dipole-dipole interaction between the two holes and using a value of $\Delta B = 16.7$ mT for the difference in the field between the two sets of S = 1 lines lead to a separation distance between the holes of about 5.5 Å. Triplet spectra of the type being observed in β-Ga_2O_3, where two holes are trapped on separate oxygen ions adjacent to one cation vacancy, have been previously reported for ZnO, Al_2O_3, and MgO crystals.[19–23]

In conclusion, we report the initial observations of the doubly ionized and singly ionized gallium vacancies in a bulk β-Ga_2O_3 crystal. The unpaired spin (i.e., the hole) in the doubly ionized V_{Ga}^{2-} charge state is localized on one threefold-coordinated oxygen adjacent to a gallium vacancy at a sixfold-coordinated gallium site. The resolved hyperfine structure present in the EPR spectra is due to interactions with the ^{69}Ga and ^{71}Ga nuclei located at the remaining two gallium neighbors next to the oxygen ion. The singly ionized V_{Ga}^{-} charge state is an S = 1 triplet state with the two holes separately localized on oxygen ions on opposite sides of the

gallium vacancy. The high degree of localization of each hole on one oxygen ion and the accompanying lattice relaxation suggest that doubly ionized and singly ionized gallium vacancies may not be shallow acceptors. It remains to be determined whether the neutral gallium vacancy in β-Ga_2O_3 has a sufficiently shallow level to produce useful *p*-type material.

This work was partially supported by Kenneth C. Goretta and the GHz-THz Electronics portfolio of the Air Force Office of Scientific Research (AFOSR). The views expressed in this paper are those of the authors and do not necessarily reflect the official policy or position of the Air Force, the Department of Defense, or the United States Government.

[1]S. I. Stepanov, V. I. Nikolaev, V. E. Bougrov, and A. E. Romanov, Rev. Adv. Mater. Sci. **44**, 63 (2016).
[2]M. Higashiwaki, K. Sasaki, H. Murakami, Y. Kumagai, A. Koukitu, A. Kuramata, T. Masui, and S. Yamakoshi, Semicond. Sci. Technol. **31**, 034001 (2016).
[3]N. T. Son, K. Goto, K. Nomura, Q. T. Thieu, R. Togashi, H. Murakami, Y. Kumagai, A. Kuramata, M. Higashiwaki, A. Koukitu, S. Yamakoshi, B. Monemar, and E. Janzén, J. Appl. Phys. **120**, 235703 (2016).
[4]K. Irmscher, Z. Galazka, M. Pietsch, R. Uecker, and R. Fornari, J. Appl. Phys. **110**, 063720 (2011).
[5]J. B. Varley, J. R. Weber, A. Janotti, and C. G. Van de Walle, Appl. Phys. Lett. **97**, 142106 (2010).
[6]J. B. Varley, H. Peelaers, A. Janotti, and C. G. Van de Walle, J. Phys.: Condens. Matter **23**, 334212 (2011).
[7]J. B. Varley, A. Janotti, C. Franchini, and C. G. Van de Walle, Phys. Rev. B **85**, 081109(R) (2012).
[8]T. Zacherle, P. C. Schmidt, and M. Martin, Phys. Rev. B **87**, 235206 (2013).
[9]S. Geller, J. Chem. Phys. **33**, 676 (1960).
[10]J. Åhman, G. Svensson, and J. Albertsson, Acta Crystallogr. C **52**, 1336 (1996).
[11]M. S. Holston, E. M. Golden, B. E. Kananen, J. W. McClory, N. C. Giles, and L. E. Halliburton, J. Appl. Phys. **119**, 145701 (2016).
[12]N. J. Stone, At. Data Nucl. Data Tables **90**, 75 (2005).
[13]M. S. Holston, J. W. McClory, N. C. Giles, and L. E. Halliburton, J. Lumin. **160**, 43 (2015).
[14]J. A. Weil and J. R. Bolton, *Electron Paramagnetic Resonance: Elementary Theory and Practical Applications*, 2nd ed. (John Wiley and Sons, Hoboken, New Jersey, 2007), Chap. 4, pp. 108–109.
[15]R. H. Bartram, C. E. Swenberg, and J. T. Fournier, Phys. Rev. **139**, A941 (1965).
[16]O. F. Schirmer, J. Phys.: Condens. Matter **18**, R667 (2006).
[17]J. Owen and E. A. Harris, "Pair spectra and exchange interactions," in *Electron Paramagnetic Resonance*, edited by S. Geschwind (Plenum Press, New York, 1972), Chap. 6, pp. 456–457.
[18]A. T. Brant, E. M. Golden, N. C. Giles, S. Yang, M. A. R. Sarker, S. Watauchi, M. Nagao, I. Tanaka, D. A. Tryk, A. Manivannan, and L. E. Halliburton, Phys. Rev. B **89**, 115206 (2014).
[19]D. Galland and A. Herve, Phys. Lett. A **33**, 1 (1970).
[20]S. M. Evans, N. C. Giles, L. E. Halliburton, and L. A. Kappers, J. Appl. Phys. **103**, 043710 (2008).
[21]R. T. Cox, Solid State Commun. **9**, 1989 (1971).
[22]K. H. Lee, G. E. Holmberg, and J. H. Crawford, Solid State Commun. **20**, 183 (1976).
[23]B. H. Rose and L. E. Halliburton, J. Phys. C: Solid State Phys. **7**, 3981 (1974).